A simplified model of the Human Immune System response to the COVID-19

Maicom Peters Xavier[1], Ruy F. Reis[2], Rodrigo W. dos Santos[3] and Marcelo Lobosco[4]
Programa de Pós-Graduação em Modelagem Computacional
Universidade Federal de Juiz de Fora
Juiz de Fora, Brazil
maicompx@gmail.com[1], ruyfreitas@ice.ufjf.br[2], marcelo.lobosco[4], rodrigo.weber@ufjf.edu.br[3]

2020 IEEE International Conference on Bioinformatics and Biomedicine (BIBM) 978-1-7281-6215-7/20/$31.00 ©2020 IEEE DOI: 10.1109/BIBM49941.2020.9313418

***Abstract*—By November 2020, the Coronavirus disease 2019 (COVID-19) has infected more than 50 million people worldwide, causing more than 1.2 million deaths. This new contagious disease is not well understood, and the scientific community is trying to comprehend better the interactions of the causative agent of the disease, SAR2-CoV-2, and the immune response to identify its weak points to develop new therapies to impair its lethal effects. Mathematical and computational tools can help in this task: the multiscale interactions among the various components of the human immune system and the pathogen are very complex. In this work, we present a simple system of five ordinary differential equations that can be used to model the immune response to SARS-CoV-2. The model parameters and initial conditions were adjusted to cohort studies that collected viremia and antibody data. The results have shown that the model was able to reproduce both viremia and antibodies dynamics successfully.**

***Index Terms*—Computational immunology, mathematical modelling, COVID-19, SARS-CoV-2.**

I. Introduction

The human body has two types of immune response against any external antigens, the innate and the adaptive (or acquired). The innate response to an external invader begins with the imposition of physical barriers to block the invasion. The first line of defense of the HIS against invaders comprises epithelial tissues and mucous membranes that line our digestive, respiratory, and reproductive tracts. When an invading antigen breaches these physical barriers, the second line of defense, composed of phagocytic cells, is ready to react. These cells play the role of eliminating antigens and dead cells through phagocytosis (a process in which the cell encompasses and digests substances in the body)[1]. The main phagocytes of HIS are macrophages, neutrophils, monocytes, and dendritic cells.

When the innate system cannot eliminate the infection caused by the invading antigens, especially by viruses, the adaptive immune system begins to develop mechanisms to fight them and thus control the infection [2]. The innate system is responsible for capturing and presenting the antigens to the adaptive immune system cells which activate this system. After the activation of B cells, which is a type of adaptive immune system cells, the production of antibodies starts. Antibodies are proteins that bind to the surface of antigens, facilitating the process of phagocytosis by the body's defense cells.

There are four main classes of antibodies: the Immunoglobulins M, A, G, and E (IgM, IgA, IgG, and IgE, respectively) [1]. IgG and IgM antibodies are very good at neutralizing and opsonizing virus: antibodies can form a bridge between the invader and the phagocyte, bringing the invader in close, and preparing it for phagocytosis [1]. IgG is the longest-lived antibody class, with a half-life of about three weeks and IgM antibodies have a half-life of only about one day [1]. Exposure to an antigen induces memory cells' production so that subsequent responses to the same antigen are faster than the first one. Other adaptive immune cells are also activated, such as T cells, which can kill cells infected by the pathogens [2], [1].

Although the adaptive immune system, in theory, can adapt to protect humans against almost any invader, in practice, this can be a challenging task, such as in the case of the SARS-CoV-2 virus. This virus belongs to the genus *Coronavirus* and causes the Coronavirus Disease 2019 (COVID-19), a severe acute respiratory syndrome. COVID-19 most likely originated in China with indications that the onset of the infection occurred in the city of Wuhan - China, in December 2019 [3], [4], [5]. As it is a new, lethal, and easily contagious/spread disease, there is an urgent need to develop an efficient vaccine and palliative care for symptoms. In cases where the disease progresses to a severe clinical condition, hospitalization of patients and even the use of ventilator support are necessary. The symptoms are diverse, such as shortness of breath, diarrhea, headaches, sore throat, gastrointestinal problems, chest pain or pressure, and loss of movement [6], [7], [8].

Due to the numerous multiscale interactions between the various components of the HIS, understanding its dynamics becomes a difficult task. In this context, computational modeling is a useful tool that can provide essential insights into this complex system. A computational model (CM), after verified and validated, can be used to answer several questions regarding the physical/biological system's behavior under different scenarios. Before starting the development of a CM, it is necessary to define which aspects are relevant to evaluate. For example, aided by a CM of the immune response to COVID-19, someone may use it to estimate the

concentration of the SARS-CoV-2 specific antibody after the onset of infection or vaccination and check for seroconversion.

This work employs a system of ODEs (Ordinary Differential Equations) to simulate the behavior of the HIS against the SARS-CoV-2 virus using a deterministic approach. Furthermore, it aims to represent the relationship between viremia caused by SARS-CoV-2 and the production of antibodies, specifically the IgG, as this is one of the principal indicators of long-term protection. The idea is to keep the model as simple as possible, with a reduced set of parameters, since many details about the disease are still unknown. This model represents a first step towards developing a stochastic model that aims to represent, in the near future, key aspects related to the development of immune memory to answer questions such as: What is the expected seroconversion rates of a COVID-19 vaccine? What are the factors that may explain why some individuals that will receive the vaccine will not seroconvert? How can the seroconversion rates be increased?

The remainder of the paper is organized as follows. Section II briefly presents some related work. Section III presents the mathematical model. The results are presented in Section IV and finally Section V presents our conclusions and plans for future work.

II. Related Work

The literature is plenty of examples of the use of CMs to model HIS using distinct techniques. The technique used depends on some important factors, such as whether a deterministic or stochastic approach will be used, whether it will be a continuous or discrete model, in addition to defining the importance of temporal or spatial evolution. Although a CM based on ordinary differential equations (ODE) can be used to describe the behavior of the HIS and the interactions between its cells and molecules over time [9], [10], [11], [12], [13], [14], and partial differential equations (PDEs) can be used to analyze the immune system spatial evolution over time [15], [16], [17], [18], [19], other approaches can also be used, such as those based on stochastic methods [20], [21], cellular automaton and agents [22], [23], [24], [25], [26].

The development of models to describe the dynamics of SARS-CoV-2 are in its beginning, with very few models available in the literature [27], [28], [29]. These works are based on the target cell-limited model [30]: a system of three ODEs to model target cells, infected cells, and viruses. In this work, we use a set of five ODEs to model not only the virus but also the B cells and IgG antibodies, comparing both the virus and IgG concentration to values found in the literature.

Du and Yan [27] developed a CM to investigate the dynamics of the immune response to influenza and to the SARS-CoV-2 virus. The adaptive system CD8+ cells, IgM and IgG antibodies are represented as constants in the model. Their numerical results suggest that the innate immune system is the main responsible for clearing the influenza virus, while the adaptive system is the main responsible for controlling the SARS-CoV-2 virus. The peak concentration of the adaptive immune cells for patients with COVID-19 is more likely to occur before the number of infected cells by SAR-CoV-2 reaches its peak [27]. Unfortunately, the authors do not present any validation of their numerical results that focus on the viral load. Afterward, the model has been modified to model the effects of a hypothetical antiviral drug on the SARS-Cov-2 infection.

The work of Hernandez-Vargas and Velasco-Hernandez [28] uses a model similar to Du and Yan [27], but including latent cells. The idea is that newly infected cells spend time in a latent phase, a concept similar to the "Eclipse Phase" [31]. Furthermore, instead of a constant [27], T cells are represented by an equation. Then, the viral load obtained by the numerical experiments is compared to values found in the literature [32], with good fitness between numerical and experimental results. The authors then present the Stability Analysis of their model [29], which suggests that the SARS-CoV-2 virus replicates fast enough to overcome T cell response and cause infection.

In one previous work, we have proposed a stochastic approach [21], based on Gillespie's algorithm [33], [34], to simulate the immune response to the Yellow Fever vaccine. The deterministic model is a system of five ODEs that represents the behavior of the following populations: Yellow Fever vaccine virus, generic antibodies, and three types of lymphocyte B cells (naive, active, and memory). Then, this model was solved using Gillespie's stochastic approach. In this work, we adapted this model to reproduce the immune response to COVID-19. We have also adjusted their parameters and initial conditions to reproduce the experimental data associated with the COVID-19, more specifically, viremia and IgG concentrations [35], [36].

III. Methods

This section presents the CM used to represent the immune response to COVID-19, the method used to adjust their parameters and initial conditions to data available in the literature, and its computational implementation.

A. Mathematical model

The mathematical model is composed by a set of five ODEs, that represents the following populations: SARS-CoV-2 virus (V), IgG antibodies(IgG), and three types of lymphocyte B cells (naive, active, and memory, represented by B_N, B_A and B_M).

Equation (1) represents the virus (V) dynamics:

$$\frac{d}{dt}V = C_1 V - C_2 V IgG. \tag{1}$$

SARS-CoV-2 uses the cell surface receptor ACE2 to infect healthy cells [37]. After the virus enters the cell, it uses cell mechanism to self-replicate. The new produced virions leave the cell to infect the nearby uninfected cells. This viral replication is represented by an exponential growth, *i.e.*, the term $C_1 V$ in Equation (1), where C_1 represents the growth rate. The term $C_2 V IgG$ denotes the viral clearance done with the help of neutralization and opsonization by IgG antibodies, where C_2 represents the clearance rate. We adopt some simplifications in this equation. First, the viral replication includes,

in a implicit way, the viral clearance done by both innate and adaptive immune cells. Usually infected cells are induced to undergo apoptosis by T killer cells, attracting macrophages and neutrophils to phagocyte them and contributing to the mitigation of the disease [38]. The second simplification is that the antibody does not kill the virus, but opsonizes it. After the antibody binds to the membrane of the virus, phagocytes are attracted to phagocyte the pathogen.

The naive B cells are represented by Equation (2):

$$\frac{d}{dt}B_N = C_3(B_{N_0} - B_N) - C_4 V B_N. \quad (2)$$

Both innate and adaptive immune cells operate under strict homeostatic controls, *i.e.*, there are relatively constant pool sizes of their naive populations that are kept by the body [39]. In the case of B_N cells, their production is done in the bone marrow. To model this homeostatic control of naive B cells, the term $C_3(B_{N_0} - B_N)$ was introduced, where B_{N_0} denotes the equilibrium population and C_3 the homeostasis rate, *i.e.*, how fast/slow the homeostasis is achieved. After B cells are produced and mature in the bone marrow, they migrate to the secondary lymphoid organs, such as the spleen and lymph nodes. Naive B cells can activate if their surface binds to the antigen they recognize. In this work, we do not consider all aspects required to activate B cells, such as the need for co-stimulatory signals by T-cells or cytokines [1]. The activation is very important because active B cells are responsible for producing antibodies. The activation is represented by the term $C_4 V B_N$, where C_4 represents the activation rate.

Equation (3) represents the active B cells:

$$\frac{d}{dt}B_A = C_4 V B_N - C_5 B_A - C_6 B_A. \quad (3)$$

A portion of the active B cells is retained within a memory poll and is important to respond faster to a second exposure to the same cognate antigen [1]. The term $C_5 B_A$ denotes the portions of active B cells that differentiate into memory cells, where C_5 is the differentiation rate. The term $C_6 B_A$ denotes the natural decay of the active B cells and C_6 is the decay rate.

Equation (4) models the memory cells:

$$\frac{d}{dt}B_M = C_5 B_A + C_7 B_M \left(1 - \frac{B_M}{B_{Mmax}}\right) - C_8 B_M. \quad (4)$$

Memory B cells constantly replicate to guarantee a long-term immunological memory, and persists for long periods of time at a relatively stable numbers [40]. The term $C_7 B_M \left(1 - \frac{B_M}{B_{Mmax}}\right)$ represents the memory B cell replication, where C_7 represents the growth rate, and B_{Mmax} limits the growth. The immunologic memory related to B cells consists of two different cell types, memory B cells and long-lived plasma cells. Long-lived plasma cells continuously secrete antibodies. Memory B cells are those that are waiting for re-exposure to the same antigen to activate. However, we adopt a simplification, in which memory B cells plays both roles. There are also two modifications in this equation compared to the original work [21], which are the removal of B_A from the memory B cell replication term, and the inclusion of the term $C_8 B_M$ to represent the natural decay of the memory cells.

Finally, Equation (5) represents the IgG antibodies:

$$\frac{d}{dt}IgG = C_9 B_M - C_{10} IgG. \quad (5)$$

Antibodies are produced by long-lived plasma B cells, but due to the simplification just explained, we assume that B_M cells produce antibodies. The term $C_9 B_M$ represent antibodies production by memory cells. The term $C_{10} IgG$ refers to the IgG antibodies natural decay at a rate equals to C_{10}.

B. Experimental Data

In order to evaluate our CM model, a set of data collected from two distinct papers that present cohort studies with people infected with SARS-CoV-2 was used.

The first paper presents temporal profile of serial viral load from a set of 23 patients admitted at two hospitals in Hong Kong, all of them with laboratory-confirmed COVID-19 [35]. Most viral load data reported in the paper were collected from posterior oropharyngeal saliva samples, except for three intubated patients, in whom viral load data were obtained from endotracheal aspirates. The work reports the mean values for samples collected daily during a period of 29 days. The number of patients who provided a sample on each day varies from one to ten. In this work, we have used only the values collected from posterior oropharyngeal saliva samples. Data were extracted from the paper using the WebPlotDigitalizer tool [41]. WebPlotDigitizer is a on-line toll that can extract data in a semi-automatic way from graphs that are uploaded to the website. Since data are extracted from an image, some small errors can be introduced in this process.

The second paper presents antibody responses to SARS-CoV-2 [36]. A cohort composed by 285 Chinese patients, all of them confirmed to be infected with SARS-CoV-2 by RT–PCR assays, were enrolled in this study from three hospitals. To measure the level of IgG and IgM against SARS-CoV-2, serum samples were collected at four different time intervals after symptom onset were reported [36]. Antibody levels were measured using magnetic chemiluminescence, which provides values divided by the cutoff (S/CO) [36], and were calculated as $log2(S/CO + 1)$. The number of patients who provided a sample on each time interval varies from seven to one hundred and thirty. The dataset is available for download, eliminating the occurrence of errors due to the data extraction process.

In both cases, data are collected after patients has been admitted at the hospital. This imposes an additional challenge because the exact day patients has been infected is not clear. Epidemiological studies carried with 425 laboratory-confirmed COVID-19 cases in Wuhan, China, have estimated that the mean incubation period is 5.2 days [5]. Based on this results, we consider that the infection occurred five days before patient admission, adjusting the cohort data accordingly to reflect this incubation period.

C. Model calibration

In order to adjust the model presented in the Section III-A to fit data from the cohort studies described in Section III-B, it is necessary to adjust the rates (C_1, C_2, ..., C_{10}). The initial conditions of some populations must also be adjusted, specially the initial concentration of SARS-CoV-2 virus.

To adjust the model parameters and initial conditions, the differential evolution (DE) optimization method [42] was used. Differential Evolution, as the name may suggest, is a type of evolutionary algorithm that uses mechanisms inspired by the theory of evolution, where the fittest individuals of a population, *i.e.* the ones that have the characteristics that allow them to survive longer, are the ones that produce more offspring, which in turn inherit the good traits of their parents [42], [43]. This makes the new generation more likely to survive in the future as well, and so the characteristics that allowed the population to survive in the past improves over time, generation after generation. DE makes use of different mechanisms present in nature, such as mutation, recombination and selection, to evolve a solution to a problem. In the case of this paper, the solution that will be evolved is to minimize the difference between the model curves (IgG and viremia) to the given data (relative error), as Equation (6) shows:

$$\min_{p} \left(\omega_1 R_E(V, \hat{V}) + \omega_2 R_E(IgG, \hat{IgG}) \right), \tag{6}$$

where p is the set of parameters to be estimated, ω_n is a weight, $\hat{V}(t)$ is the viremia, $\hat{IgG}(t)$ is the IgG concentration. For this work, we used $\omega_1 = \omega_2 = 1.0$, which means that DE tries to find values for the set p that minimize errors in both variables equally, *i.e.*, no variable is more important than the other. R_E represents the relative error between the cohort data and the numerical result, and is computed as follows:

$$R_E(\lambda, \hat{\lambda}) = \frac{\|\lambda(t,p) - \hat{\lambda}(t)\|_1}{\|\hat{\lambda}(t)\|_1}. \tag{7}$$

In order to speedup the convergence to a feasible solution, constraints are passed as parameters to the solver, establishing upper and lower limits to each parameter, following the approach proposed by Lampinen [44]. The intervals defined to each parameter are presented in Table I.

Other populations, such as the initial concentration of naive B cells and the upper limit of the memory B cells population, were obtained from data in the literature [45].

D. Computational model

The model was implemented in the Python programming language. Numerical solution of the system of ODEs were performed by the `odeint` function, a member of the integrate package in the `scipy` library[46], which includes libraries for solving ODEs. This function uses the characteristics of the ODE system to select the best numerical method to solve it. The function can solve the ODEs system using either the Backward Differentiation Formula (BDF) or the Adams method [47]. The function uses BDF for stiff equations and the implicit Adams method is used otherwise. The DE code was implemented in Python, using for this purpose the Numpy library ($\geq$ 1.7.0 version).

TABLE I
BASELINE VALUES USED FOR THE CALIBRATION OF THE MODEL´S PARAMETERS AND INITIAL CONDITIONS.

Parameter/Initial Condition	**Interval**
C_1	$(1.0 \times 10^{-4}, 1.0)$
C_2	$(1.0 \times 10^{-4}, 1.0)$
C_3	$(1.0 \times 10^{-4}, 1.0)$
C_4	$(1.0 \times 10^{-4}, 1.0)$
C_5	$(1.0 \times 10^{-4}, 1.0)$
C_6	$(1.0 \times 10^{-4}, 1.0)$
C_7	$(1.0 \times 10^{-4}, 1.0)$
C_8	$(1.0 \times 10^{-4}, 1.0)$
C_9	$(1.0 \times 10^{-4}, 1.0)$
C_{10}	$(1.0 \times 10^{-4}, 1.0)$
V	$(1.0 \times 10^{-2}, 1.0)$

The experiments were performed using Python version 3.7.6 64-bit using the Spyder 4.0.1 integrated development environment (IDE). The execution environment was composed of an Intel Core i5-3317U 1.7 GHz processor, with 6 GB of RAM. The system runs Windows 10 Home version 1903.

IV. RESULTS

This section presents the results obtained for the calibration of the model using DE, as well as the numerical results obtained after the parameters and initial conditions of the model have been adjusted. Finally, a brief discussion is presented.

A. Model Calibration

After fitting model's parameters and the initial value of viremia to experimental data, using the baseline values presented in Table I, we observed relative errors of approximately 40% for the virus and 21% for the antibodies curves, according to equations presented in subsection III-C.

B. Numerical Results

In order to qualitatively validate our model, the CM was used to simulate the scenario where an individual was infected by the SARS-CoV-2 virus for the first time. The numerical results obtained by the mathematical model were then compared to the viremia and IgG concentrations found in the literature [35], [36]. All the initial values used for the variables as well as the model parameters are presented in the Appendix.

Figure 1 shows the comparison between the viremia curve obtained numerically, after calibration, and experimentally. Gray dots represent average levels of viremia obtained from patients who developed COVID-19 [35], while the dark curve represents the numerical results. Experimental results are available up to 29 days after hospital admission, *i.e.*, 34 days after the infection. SARS-CoV-2 RNA could not be detected after 20 days or longer for a third of patients who survived, but in one patient the SARS-CoV-2 RNA was detected after

25 days. For this reason, we decided to simulate the equivalent of 50 days after the start of the infection.

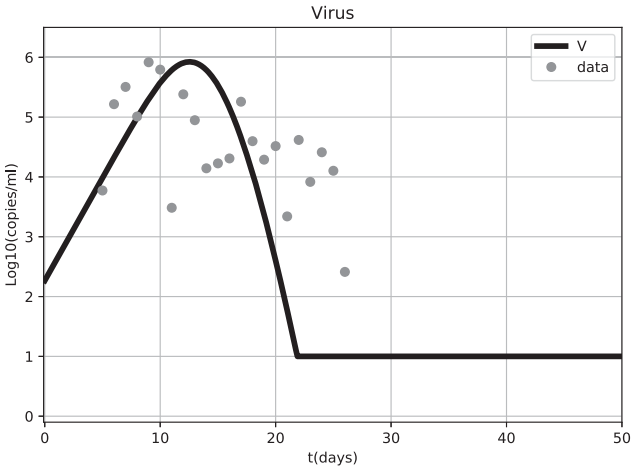

Fig. 1. Viremia curve obtained by the simulation of deterministic model presented in Section III-A, simulated using the initial conditions presented in Tables II and III. Dark curve represent the numerical results and the gray dots experimental data [35].

Figure 2 presents the comparison between the IgG curve obtained numerically, after calibration, and experimentally. Gray dots represent average IgG antibody titers obtained from patients [36], while the dark curve represents the numerical results. Although experimental results are available up to 27 days after hospital admission, *i.e.*, 31 days after the infection, we decided to simulate the equivalent of 200 days after infection to better observe the behavior of the curve, specially if a plateau or slow decay could be found.

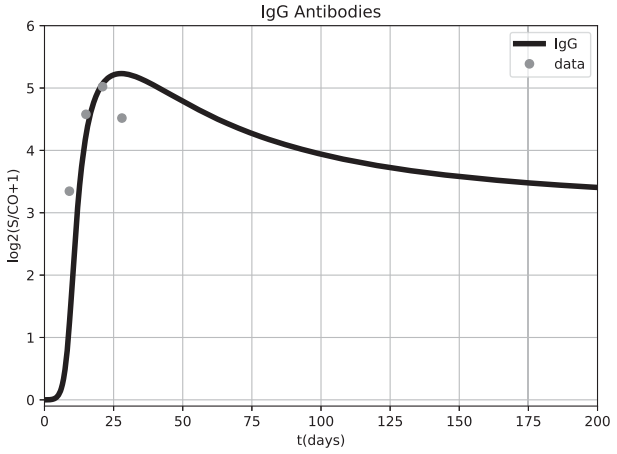

Fig. 2. IgG curve obtained by the simulation of deterministic model presented in Section III-A, simulated using the initial conditions presented in Tables II and III. Dark curve represent the numerical results and the gray dots experimental data [36]

Unfortunately we do not have experimental data for other populations of the model (B cells) and, for this reason, we do not present their results in this section. Furthermore, the comparison would be complex because of the simplifications adopted in this work; for example, B memory cells acts as both long-lived plasma cells and B memory cells.

C. Discussion

As one can observe in Figure 1, the CM obtained good results from a qualitative perspective. It should be mentioned that the experimental data presents a huge variation (observe that the scale adopted is $\log_{10}$), impairing the adjust reported in Section IV-A. Perhaps this could be explained by the severity of the disease: the literature reports that the viremia peak depends on it, with severe/critical patients tending to peak in the second week of illness, with values ranging from 5.57–9.66 $\log_{10}$ copies/mL, while in mild/moderate patients the viral load peak is observed in the first week of illness, with values ranging from 3.25–6.40 $\log_{10}$ copies/mL [48]. So one possible explanation for the huge variation observed in the viremia is that the dataset mixes patients with distinct degrees of disease severity. In such a case, the numerical results represent an average value for distinct severity degrees. There are some evidences of the prevalence of severe/critical patients in the dataset, not only due to the need of hospital admission, but also to the fact that the viremia peak observed in the numerical result occurs about the fifteenth day, with a value about 6 $\log_{10}$ copies/mL, values compatible with the one reported for severe/critical patients [48].

As one can observe in Figure 2, antibody titers follow the classic pattern observed in antibody curves, with a rapid increase within the first three weeks after symptoms [49]. Furthermore, the model was able to reproduce experimental data, achieving almost the same peak value and date of peak. The IgG curve suggests that the antibodies remain detectable up to six months after infection. This behavior is the same described in the literature [49].

COVID-19 is a new disease and, for this reason, some studies and datasets seems to contradict each other. Furthermore, the experimental data used in this paper to adjust the model are composed by few patients. For some days, data of a single patient was used in the adjusts. Distinct studies in the literature adopts distinct methods and metrics, so it is not easy to gather their data together in a single dataset with a large number of patients. In this sense, the results presented in this work have limitations due to the restrictions imposed by data availability.

V. Conclusion

This paper evaluated a simple mathematical model, composed by a set of five ordinary differential equations, to model the immune response to SARS-CoV-2. The model parameters and initial conditions were successfully adjusted using Differential Evolution to fit viremia and IgG curves obtained in two distinct cohort studies. The dynamics of the disease were reproduced qualitatively: the values related with viremia and IgG peaks (not only the value, but also the approximate day in which it occurred) were close to the values obtained numerically. In the numerical simulations, the peak of viremia occurred approximately fifteen days after the infection and the level of antibodies increases rapidly during the first three weeks after infection, remaining present up to six months.

The results presented in this work have limitations due to the restrictions imposed by data availability, specially due to the small number of individuals used in some adjusts. We expect that, in future works, more data are available to improve our results. We also plan to include other populations, like citokynes, since the literature describes that the severe deterioration of some patients has been closely related to the occurrence of a citokyne storm.

The search to find a vaccine for the SARS-CoV-2 is well underway, with many distinct groups announcing the Phase 3 COVID-19 vaccine candidate studies. As future works, we plan to use a stochastic version of this model to simulate the immune response the vaccine, in order to answer questions such as: What is the expected seroconversion rates of a COVID-19 vaccine? What are the factors that may explain why some individuals that will receive the vaccine will not seroconvert? How can the seroconversion rates be increased?

ACKNOWLEDGMENT

The authors would like to express their thanks to CAPES, CNPq, FAPEMIG and UFJF for funding this work.

APPENDIX A
INITIAL CONDITION AND PARAMETERS USED IN THE SIMULATIONS

TABLE II
VARIABLES AND THEIR INITIAL VALUES.

Variable	Description	Initial value
V	SARS-CoV-2	$2.3log_{10}(copies/ml)$
B	Naive B cells	$2.5 \times 10^5(cells/ml)$
B_A	Active B cells	0 (cells/ml)
B_M	Memory B cells	0 (cells/ml)
IgG	IgG antibodies	0 (S/CO)

TABLE III
PARAMETERS AND THEIR VALUES.

Parameter	Value
C_1	$7.9 \times 10^{-1}(day^{-1})$
C_2	$8.5 \times 10^{-2}(day^{-1}(S/CO)^{-1})$
C_3	$3.6 \times 10^{-3}(day^{-1})$
C_4	$2.1 \times 10^{-6}(day^{-1}(copies/ml)^{-1})$
C_5	$8.6 \times 10^{-2}(day^{-1})$
C_6	$9.0 \times 10^{-3}(day^{-1})$
C_7	$1.1 \times 10^{-2}(day^{-1})$
C_8	$3.1 \times 10^{-4}(day^{-1})$
C_9	$1.2 \times 10^{-4}(day^{-1})$
C_{10}	$4.5 \times 10^{-1}(day^{-1})$
B_{Mmax}	$3.5 \times 10^4(cells/ml)$

REFERENCES

[1] L. M. Sompayrac, *How the immune system works*. John Wiley & Sons, 2015.

[2] A. K. Abbas, A. H. Lichtman, and S. Pillai, *Basic Immunology: Functions and Disorders of the Immune System*. Elsevier Health Sciences, 2019.

[3] N. Zhu, D. Zhang, W. Wang, X. Li, B. Yang, J. Song, X. Zhao, B. Huang, W. Shi, R. Lu *et al.*, "A novel coronavirus from patients with pneumonia in china, 2019," *New England Journal of Medicine*, 2020.

[4] F. Wu, S. Zhao, B. Yu, Y.-M. Chen, W. Wang, Z.-G. Song, Y. Hu, Z.-W. Tao, J.-H. Tian, Y.-Y. Pei *et al.*, "A new coronavirus associated with human respiratory disease in china," *Nature*, vol. 579, no. 7798, pp. 265–269, 2020.

[5] Q. Li, X. Guan, P. Wu, X. Wang, L. Zhou, Y. Tong, R. Ren, K. S. Leung, E. H. Lau, J. Y. Wong *et al.*, "Early transmission dynamics in wuhan, china, of novel coronavirus–infected pneumonia," *New England Journal of Medicine*, 2020.

[6] C. Huang, Y. Wang, X. Li, L. Ren, J. Zhao, Y. Hu, L. Zhang, G. Fan, J. Xu, X. Gu *et al.*, "Clinical features of patients infected with 2019 novel coronavirus in wuhan, china," *The lancet*, vol. 395, no. 10223, pp. 497–506, 2020.

[7] N. Chen, M. Zhou, X. Dong, J. Qu, F. Gong, Y. Han, Y. Qiu, J. Wang, Y. Liu, Y. Wei *et al.*, "Epidemiological and clinical characteristics of 99 cases of 2019 novel coronavirus pneumonia in wuhan, china: a descriptive study," *The Lancet*, vol. 395, no. 10223, pp. 507–513, 2020.

[8] Y.-Y. Zheng, Y.-T. Ma, J.-Y. Zhang, and X. Xie, "Covid-19 and the cardiovascular system," *Nature Reviews Cardiology*, vol. 17, no. 5, pp. 259–260, 2020.

[9] A. S. Perelson, "Modeling the interaction of the immune system with hiv," in *Mathematical and statistical approaches to AIDS epidemiology*. Springer, 1989, pp. 350–370.

[10] C. Baker, G. Bocharov, and C. Paul, "Mathematical modelling of the interleukin-2 t-cell system: A comparative study of approaches based on ordinary and delay differential equation," *Computational and Mathematical Methods in Medicine*, vol. 1, no. 2, pp. 117–128, 1997.

[11] S. T. Chang, J. J. Linderman, and D. E. Kirschner, "Multiple mechanisms allow mycobacterium tuberculosis to continuously inhibit mhc class ii-mediated antigen presentation by macrophages," *Proceedings of the National Academy of Sciences of the United States of America*, vol. 102, no. 12, pp. 4530–4535, 2005.

[12] Y. Vodovotz, C. C. Chow, J. Bartels, C. Lagoa, J. M. Prince, R. M. Levy, R. Kumar, J. Day, J. Rubin, G. Constantine *et al.*, "In silico models of acute inflammation in animals," *Shock*, vol. 26, no. 3, pp. 235–244, 2006.

[13] C. Bonin, R. W. dos Santos, G. Fernandes, and M. Lobosco, "Computational modeling of the immune response to yellow fever," *Journal of Computational and Applied Mathematics*, vol. 295, pp. 127–138, 2016.

[14] ——, "A simplified mathematical-computational model of the immune response to the yellow fever vaccine," in *Bioinformatics and Biomedicine (BIBM), 2017 IEEE International Conference on*. IEEE, 2017, p. to appear.

[15] G. Pettet, H. Byrne, D. McElwain, and J. Norbury, "A model of wound-healing angiogenesis in soft tissue," *Mathematical biosciences*, vol. 136, no. 1, pp. 35–63, 1996.

[16] B. Su, W. Zhou, K. Dorman, and D. Jones, "Mathematical modelling of immune response in tissues," *Computational and Mathematical Methods in Medicine*, vol. 10, no. 1, pp. 9–38, 2009.

[17] J. A. Flegg, H. M. Byrne, M. B. Flegg, and D. S. McElwain, "Wound healing angiogenesis: the clinical implications of a simple mathematical model," *Journal of theoretical biology*, vol. 300, pp. 309–316, 2012.

[18] A. B. Pigozzo, G. C. Macedo, R. W. Dos Santos, and M. Lobosco, "On the computational modeling of the innate immune system," *BMC bioinformatics*, vol. 14, no. 6, p. S7, 2013.

[19] B. d. M. Quintela, R. W. dos Santos, and M. Lobosco, "On the coupling of two models of the human immune response to an antigen," *BioMed research international*, vol. 2014, 2014.

[20] D. L. Chao, M. P. Davenport, S. Forrest, and A. S. Perelson, "A stochastic model of cytotoxic t cell responses," *Journal of Theoretical Biology*, vol. 228, no. 2, pp. 227–240, 2004.

[21] M. P. Xavier, C. R. Bonin, R. W. dos Santos, and M. Lobosco, "On the use of gillespie stochastic simulation algorithm in a model of the human immune system response to the yellow fever vaccine," in *2017 IEEE International Conference on Bioinformatics and Biomedicine (BIBM)*, vol. 00, Nov. 2017, pp. 1476–1482. [Online]. Available: doi.ieeecomputersociety.org/10.1109/BIBM.2017.8217880

[22] F. Celada and P. E. Seiden, "A computer model of cellular interactions in the immune system," *Immunology today*, vol. 13, no. 2, pp. 56–62, 1992.

[23] D. Morpurgo, R. Serenthà, P. E. Seiden, and F. Celada, "Modelling thymic functions in a cellular automaton," *International immunology*, vol. 7, no. 4, pp. 505–516, 1995.

[24] B. Kohler, R. Puzone, P. E. Seiden, and F. Celada, "A systematic approach to vaccine complexity using an automaton model of the cellular and humoral immune system: I. viral characteristics and polarized responses," *Vaccine*, vol. 19, no. 7, pp. 862–876, 2000.

[25] M. Bernaschi and F. Castiglione, "Design and implementation of an immune system simulator," *Computers in Biology and Medicine*, vol. 31, no. 5, pp. 303 – 331, 2001.

[26] F. Pappalardo, G. Russo, M. Pennisi, G. Sgroi, G. A. P. Palumbo, S. Motta, D. Maimone, and F. Chiacchio, "Agent based modeling of relapsing multiple sclerosis: A possible approach to predict treatment outcome," in *2018 IEEE International Conference on Bioinformatics and Biomedicine (BIBM)*. IEEE, 2018, pp. 1380–1385.

[27] S. Q. Du and W. Yuan, "Mathematical modeling of interaction between innate and adaptive immune responses in covid-19 and implications for viral pathogenesis," *Journal of Medical Virology*, 2020.

[28] E. A. Hernandez-Vargas and J. X. Velasco-Hernandez, "In-host mathematical modelling of covid-19 in humans," *Annual reviews in control*, 2020.

[29] A. E. S. Almocera, G. Quiroz, and E. A. Hernandez-Vargas, "Stability analysis in covid-19 within-host model with immune response," *Communications in Nonlinear Science and Numerical Simulation*, p. 105584, 2020.

[30] A. S. Perelson, "Modelling viral and immune system dynamics," *Nature Reviews Immunology*, vol. 2, no. 1, pp. 28–36, 2002.

[31] C. A. Beauchemin, J. J. McSharry, G. L. Drusano, J. T. Nguyen, G. T. Went, R. M. Ribeiro, and A. S. Perelson, "Modeling amantadine treatment of influenza a virus in vitro," *Journal of theoretical biology*, vol. 254, no. 2, pp. 439–451, 2008.

[32] R. Wölfel, V. M. Corman, W. Guggemos, M. Seilmaier, S. Zange, M. A. Müller, D. Niemeyer, T. C. Jones, P. Vollmar, C. Rothe *et al.*, "Virological assessment of hospitalized patients with covid-2019," *Nature*, vol. 581, no. 7809, pp. 465–469, 2020.

[33] D. T. Gillespie, "A general method for numerically simulating the stochastic time evolution of coupled chemical reactions," *Journal of Computational Physics*, vol. 22, no. 4, pp. 403–434, Dec. 1976.

[34] ——, "Exact stochastic simulation of coupled chemical reactions," *J. Phys. Chem.*, vol. 81, no. 25, pp. 2340–2361, 1977.

[35] K. K.-W. To, O. T.-Y. Tsang, W.-S. Leung, A. R. Tam, T.-C. Wu, D. C. Lung, C. C.-Y. Yip, J.-P. Cai, J. M.-C. Chan, T. S.-H. Chik *et al.*, "Temporal profiles of viral load in posterior oropharyngeal saliva samples and serum antibody responses during infection by sars-cov-2: an observational cohort study," *The Lancet Infectious Diseases*, 2020.

[36] Q.-X. Long, B.-Z. Liu, H.-J. Deng, G.-C. Wu, K. Deng, Y.-K. Chen, P. Liao, J.-F. Qiu, Y. Lin, X.-F. Cai *et al.*, "Antibody responses to sars-cov-2 in patients with covid-19," *Nature medicine*, pp. 1–4, 2020.

[37] H. Zhang, J. Penninger, Y. Li, N. Zhong, and A. Slutsky, "Angiotensin-converting enzyme 2 (ace2) as a sars-cov-2 receptor: molecular mechanisms and potential therapeutic target," *Intensive Care Med*, vol. 46, no. 4, pp. 586–590, 2020.

[38] F. Nainu, A. Shiratsuchi, and Y. Nakanishi, "Induction of apoptosis and subsequent phagocytosis of virus-infected cells as an antiviral mechanism," *Frontiers in immunology*, vol. 8, p. 1220, 2017.

[39] J. E. Crowley, J. L. Scholz, W. J. Quinn III, J. E. Stadanlick, J. F. Treml, L. S. Treml, Y. Hao, R. Goenka, P. J. O'Neill, A. H. Matthews *et al.*, "Homeostatic control of b lymphocyte subsets," *Immunologic research*, vol. 42, no. 1-3, pp. 75–83, 2008.

[40] W. E Paul, *Fundamental Immunology*. Lippincott Williams & Wilkins, 2008.

[41] A. Rohatgi, "Webplotdigitizer: Version 4.3," 2020. [Online]. Available: https://automeris.io/WebPlotDigitizer

[42] R. Storn and K. Price, "Differential evolution–a simple and efficient heuristic for global optimization over continuous spaces," *Journal of global optimization*, vol. 11, no. 4, pp. 341–359, 1997.

[43] P. Rodriguez-Mier, "A tutorial on differential evolution with python," September 2017. [Online]. Available: https://pablormier.github.io/

[44] J. Lampinen, "A constraint handling approach for the differential evolution algorithm," in *Proceedings of the 2002 Congress on Evolutionary Computation. CEC'02 (Cat. No. 02TH8600)*, vol. 2. IEEE, 2002, pp. 1468–1473.

[45] H. Morbach, E. Eichhorn, J. Liese, and H. Girschick, "Reference values for b cell subpopulations from infancy to adulthood," *Clinical & Experimental Immunology*, vol. 162, no. 2, pp. 271–279, 2010.

[46] Odeint, "Odeint's homepage," November 2020. [Online]. Available: http://docs.scipy.org

[47] R. J. LeVeque, *Finite difference methods for ordinary and partial differential equations - steady-state and time-dependent problems*. SIAM, 2007.

[48] G. Lui, L. Ling, C. K. Lai, E. Y. Tso, K. S. Fung, V. Chan, T. H. Ho, F. Luk, Z. Chen, J. K. Ng *et al.*, "Viral dynamics of sars-cov-2 across a spectrum of disease severity in covid-19," *The Journal of Infection*, 2020.

[49] P. Figueiredo-Campos, B. Blankenhaus, C. Mota, A. Gomes, M. Serrano, S. Ariotti, C. Costa, H. Nunes-Cabaço, A. M. Mendes, P. Gaspar *et al.*, "Seroprevalence of anti-sars-cov-2 antibodies in covid-19 patients and healthy volunteers up to six months post disease onset," *European journal of immunology*, 2020.